

# On-Orbit Observations of Conjoining Space Objects Prior to the Time of Closest Approach

**Robert ‘Lauchie’ Scott, PhD**

Defence R&D Canada Ottawa, 3701 Carling Avenue, Ottawa, ON, K1A 0Z4

**Stefan Thorsteinson, M.Sc.**

Calian Inc. 340 Legget Drive, Ottawa, ON, Canada, K2K 1Y6

**Viqar Abbasi, M.Eng.**

Canadian Space Agency – 6767 Route d’Aéroport, St. Hubert, QC, Canada, J3Y 8Y9

## ABSTRACT

Conjunction assessment of space objects in Low Earth Orbit (LEO) generally uses information collected by ground-based space surveillance sensors. These sensors track both the *primary* object (normally an active satellite) and the *secondary* object (typically space debris). The tracking data is used to update both objects’ orbits for collision risk assessment. The primary satellite’s involvement in this process is that of a satellite in jeopardy - the primary satellite does not usually contribute tracking data on the secondary as they are typically unequipped to do so.

In this paper, an examination how an at-risk LEO primary satellite could obtain optical tracking data on a secondary object prior to the Time of Closest Approach (TCA) and assess its own collision risk without the need for additional ground-based space surveillance data is performed. This analysis was made possible by using in-situ optical measurements of space objects conjoining with the Canadian NEOSSat Space Situational Awareness R&D microsatellite. By taking advantage of the near “constant-bearing, decreasing range” observing geometry formed during a LEO conjunction, NEOSSat can collect astrometric and photometric measurements of the secondary object in the time prior to TCA, or in the multiple half-orbits preceding TCA. This paper begins by describing the in-situ phenomenology of optically observed conjunctions in terms of the observing approach, geometry and detected astrometric and photometric characteristics. It was found that conjoining objects are detectable to magnitude 16 and astrometric observations can improve position covariances used for the computation of probability of collision. In orbits prior to TCA, in-track positioning error is improved by a factor of two or more by processing space-based observations on a filtered position estimate of the secondary. However, cross-track positioning knowledge is negligibly improved due to the inherent astrometric measurement precision of the NEOSSat sensor and the oblique observing geometry during conjunction observations.

## 1. INTRODUCTION

Satellite operators are continuing to manage the increasing number of collision (conjunction) warnings due to the growing number of debris objects in Earth orbit. In Canada, operators of space assets in Low Earth Orbit (LEO) rely on conjunction screening performed by the US Air Force’s 18<sup>th</sup> Space Control Squadron (18 SPCS) using orbital data from the Space Surveillance Network (SSN) to manage close encounters between space objects [1]. For LEO operators in 18 SPCS Advanced Screening service [1,2], conjunction warnings are usually forecasted up to 7 days in advance of the Time of Closest Approach (TCA) between the two space objects and warning messages are relayed by 18 SPCS to satellite operators helping mitigate the risk of collision. These warnings take the form of Conjunction Data Messages (CDMs), a standardized format enabling rapid evaluation of collision risk of two space objects [1]. In the lead-up to TCA, space surveillance sensors acquire more tracking data to increase positioning knowledge of both objects helping validate the actual risk. Risk is generally estimated by computing the Probability of Collision (PoC) that the two space objects could collide based on the primary and secondary’s orbital position covariance and their spherical hard-body radii. In Canadian space operations a PoC exceeding  $10^{-6}$  is considered to be a “warning” criteria whereas PoCs exceeding  $10^{-4}$  are considered “action” criteria by both the Canadian Space Operations Centre (CanSpOC) and the Canadian Space Agency’s satellite operations team. For the latter, enhanced orbital analysis or debris avoidance maneuvers could be performed [2,3] to help mitigate the risk of collision.

This model of conjunction assessment works relatively well for the current population of space objects. However, this technique inherently relies on tracking data collected by ground-based sensors in the time prior to TCA. The primary satellite does not contribute to the risk assessment, nor does it collect observations on the secondary during

the days (or hours) leading up to the conjunction. The conjunction event itself is generally unobserved by Space Situational Awareness (SSA) sensors to validate that the objects safely passed one another. The collision avoidance process is also hindered by infrequent ground station accesses limiting the number of opportunities that a satellite operator can upload maneuver commands in response to new orbital data. In an era of upcoming kilo-constellations, satellite operators may not be able to provide the individual attention required for each constellation asset. This will likely make automation and independent tracking data a requirement for future space systems to help mitigate orbital collisions. In this paper, the expanded question is asked: *Can a satellite take optical observations on conjuncting space objects to independently assess the risk of collision?*

In 2018, NEOSSat, a microsatellite jointly operated by the Canadian Space Agency and Defence R&D Canada, began a series of observational experiments examining space objects conjuncting with it. The intent of this exploration was to optically characterize conjuncting space objects to see if future satellites could observe such conjunction risks to see if self-protection is a possibility if enough onboard autonomy were available. While NEOSSat does not have the on-board algorithms required to independently update a conjuncting space object’s orbit nor does it have a propulsion system to perform a debris avoidance maneuvers if a collision risk threatens, an analysis of rapid encounter observing strategies is of some value. This paper begins by describing the in-situ phenomenology of optically observed conjunctions in terms of their approach geometry, observing techniques, and the detected astrometric and photometric properties of the secondary. We then examine how a LEO satellite, equipped with an optical space surveillance sensor, could contribute to the collision avoidance process, rather than being a passive satellite-at-risk. It was found that regular observing opportunities on the secondary object occur in the *half-orbit* intersections prior to conjunction. An examination of how this half-orbit technique can be used in real-life conjunction scenarios is explored and position covariance improvements and limitations are examined.

## 2. CHARACTERISTICS OF NEOSSAT CONJUNCTIONS

NEOSSat is a 74 kg small space telescope of overall dimensions of 1.37 x 0.78 x 0.38 meters [4]. NEOSSat’s 785 km altitude orbit borders the densest part of the LEO orbital debris environment leading to regular conjunctions with a variety of payload and debris objects. The frequency of conjunction events with NEOSSat varies, but the historical average to date is ~1 conjunction event/week. Fig. 1 shows the top 40 objects frequently conjuncting with NEOSSat since its launch in 2013. Debris objects from FengYun 1C, Cosmos 2251, and Iridium 33 dominate the conjunction warnings issued to NEOSSat’s satellite operations team. Objects positively identified as *debris* constitute ~60% of NEOSSat’s conjunction history while another 7% are unknown objects not found in the public catalogs.

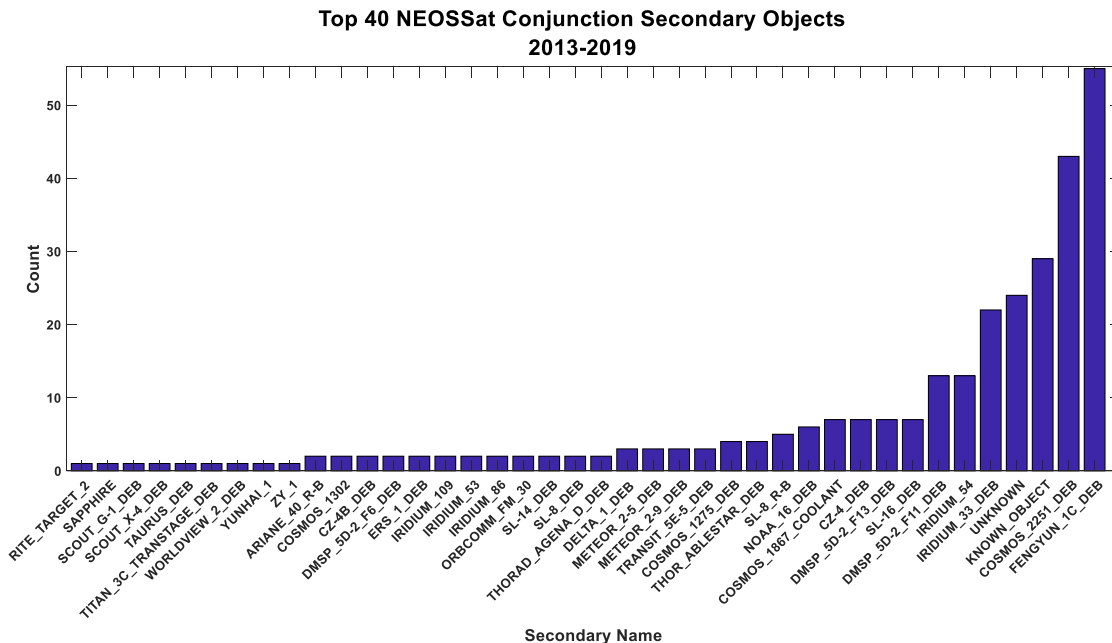


**Fig.1.** Top 40 objects conjuncting frequently with NEOSSat

Over 84% of NEOSSat's historical conjunctions had PoCs less than the Canadian Space Agency's warning criterion of  $10^{-6}$  (see Fig. 2a). The highest PoC received for NEOSSat was  $2.4 \times 10^{-4}$ . Maneuvers would generally be considered at this PoC, however NEOSSat does not have a propulsion system to perform debris avoidance. NEOSSat conjunctions tend to have overall miss distances of  $\sim 1000$  m (Fig. 2b) due to the 18 SPCS' conjunction screening algorithm examining a relatively large volume of  $1 \times 1 \times 1$  km<sup>3</sup> around NEOSSat. A smaller portion of the conjunctions have miss distances of 100-400 meters.

The radial miss distances of NEOSSat conjunctions (Fig. 2c) show some interesting features. Conjunctioning space objects tend to pass NEOSSat in three approximate altitude bands of approximately -750m, 100m and +750m with a general tendency to pass below the vehicle. This is attributed to the main secondary types - Feng Yun 1C debris, Cosmos 2251 debris, Known, Unknown and Iridium 33 debris objects.

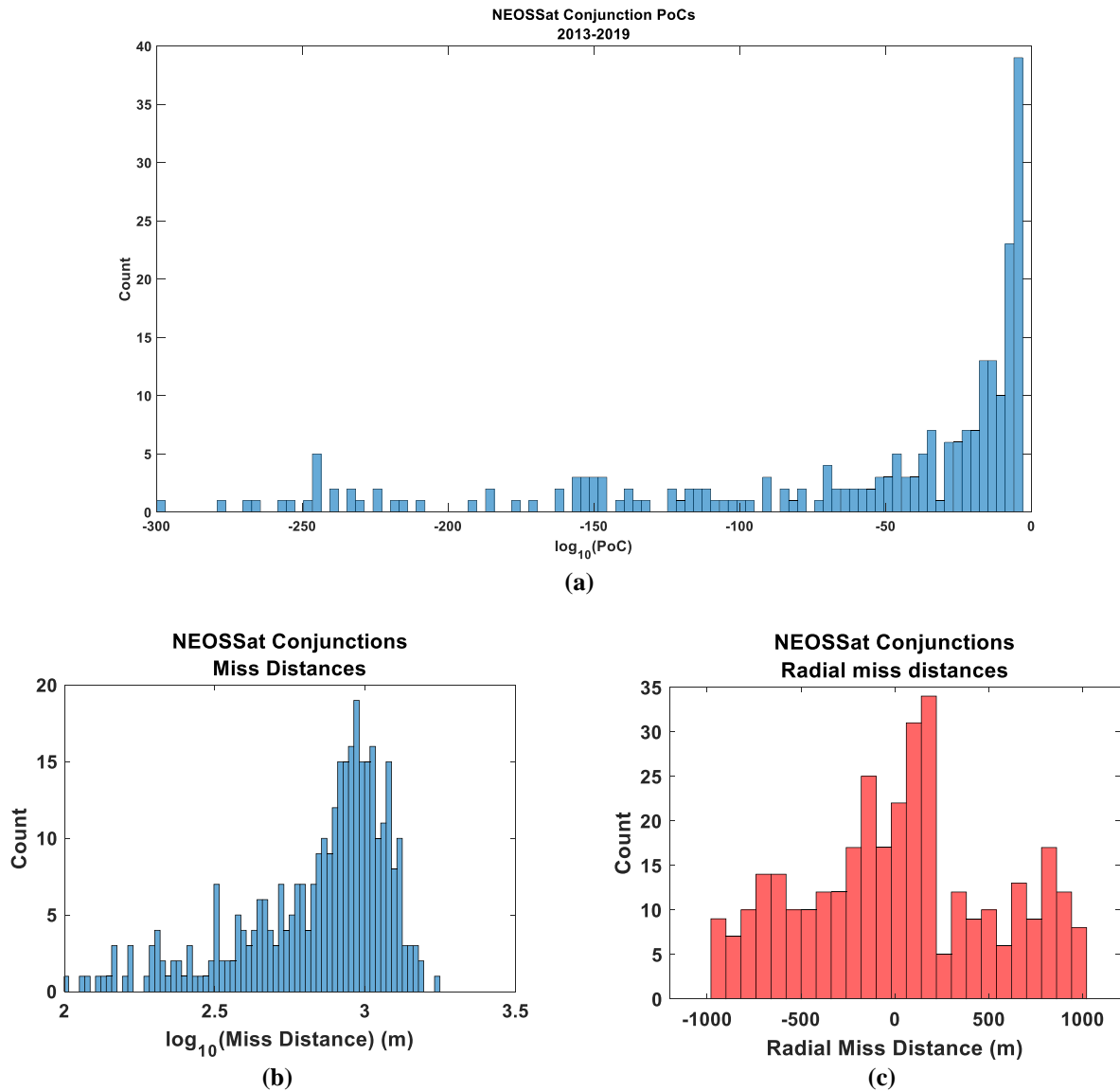


**Fig.2** (a) NEOSSat conjunction probabilities of collision. (b) Secondary object miss distances with NEOSSat, (c) Radial miss distance histogram showing the tendency of secondaries to pass below the vehicle.

NEOSSat conjunction warnings issued by 18 SPCS have a lopsided distribution of warning time, primarily driven by CSA's transition to the 18 SPCS Advanced Screening service for conjunction assessment [2]. From 2013 to 2016, 18 SPCS provided NEOSSat conjunction assessment data up to 3 days prior to TCA, causing the rise in warnings at the three-day point shown in Fig. 3. Since 2016, 18 SPCS provides conjunction screening up to seven days prior to TCA. This causes the sharp rise in warning times near 7 days. As of 2019, more than 50% of all NEOSSat conjunctions have 6 days of warning time offering the satellite operations team more time to perform analysis and trending of conjunction events and to develop in-situ conjunction imaging experiments, as described in the next section.

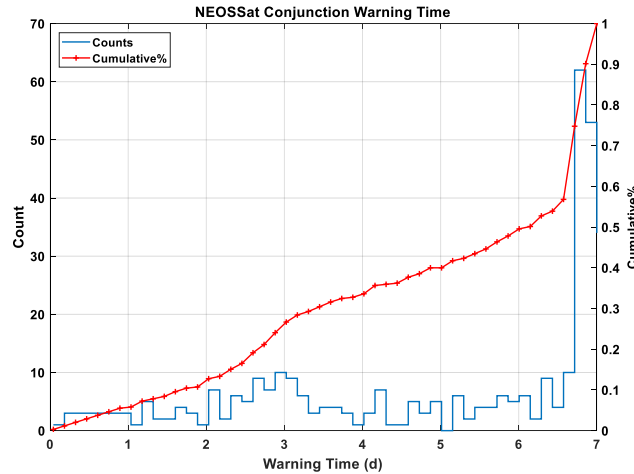


Fig.3. NEOSSat conjunction warning times (days)

### 3. IN-SITU OPTICAL CHARACTERISTICS OF LEO SATELLITE CONJUNCTIONS

In 2018, NEOSSat began its first observations of objects forecasted to pass within a few kilometers of it in LEO. During a conjunction the secondary object appears in a near *constant-bearing, decreasing range* visibility condition in the few minutes prior to TCA. The secondary object appears to have very small angular rates when observed at ranges from 4000 km down to 250 km at these times. When a secondary passes within 250 km, NEOSSat is unable to track it as its angular rate accelerates drastically at TCA exceeding NEOSSat's attitude control capabilities. The time interval leading up to TCA creates short observing windows for NEOSSat to lock onto background star fields and acquire imagery on the advancing secondary object until it drifts off-frame during its pass. Fig. 4 shows the approach geometry of the Spot-2 satellite and a NEOSSat image of its approach during a conjunction in 2018.

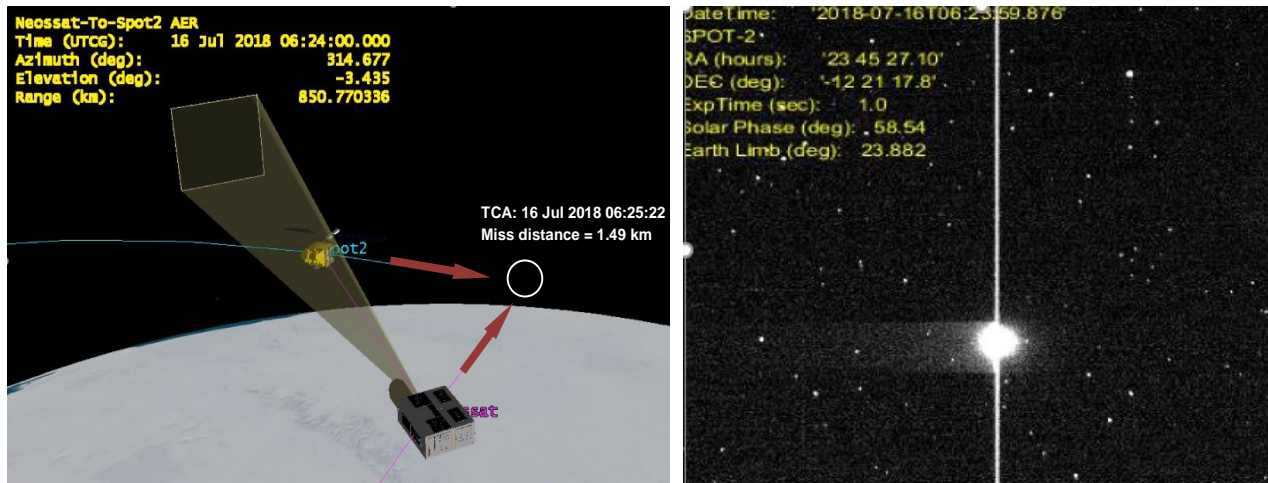


Fig.4. (Left) NEOSSat conjunction geometry with Spot-2. (Right): Single frame of Spot-2 as observed by NEOSSat

There are two key photometric properties exhibited by conjuncting objects when tracked by a LEO observer:

**Range Induced Brightening:** Conjuncting LEO objects exhibit strong, range-induced, brightening during the time leading up to TCA. Fig. 5 shows the Spot-2 satellite during its illuminated approach toward NEOSSat. Bloom spikes are seen due to NEOSSat’s CCD saturating on the bright, approaching object. Careful selection of NEOSSat’s CCD exposure time reduces the likelihood of saturation and is a key consideration when planning observations.

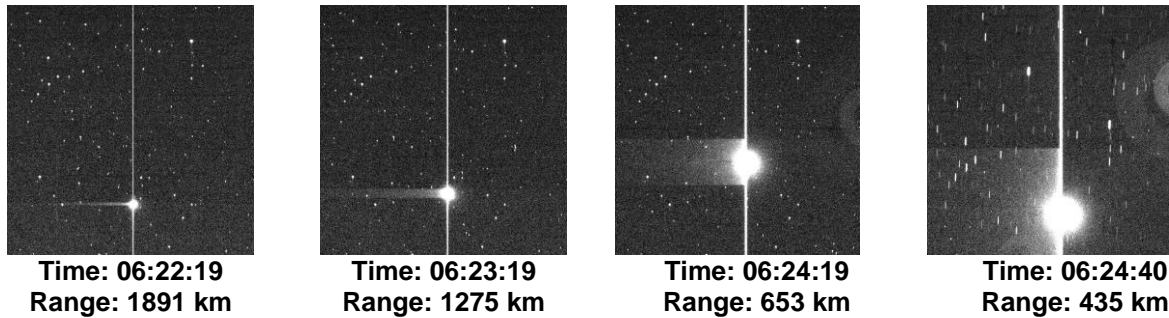


Fig.5. NEOSSat observations of the Spot-2 satellite conjunction on 16 July 2018.

**Near-Constant Phase Angles:** Conjuncting space objects observed in LEO exhibit a near constant Sun/Object/Observer phase angle geometry prior to TCA. The near-rectilinear motion of the two objects creates this quirk of conjunction geometry. This creates an operational constraint during NEOSSat observing as NEOSSat’s star tracker is designed to operate outside of a 45° exclusion angle from the Sun. This forces the majority of NEOSSat’s conjunction observations to be collected on objects during opposition or phase angles < 90°. NEOSSat can observe space objects in the Sun-ward direction but must respect NEOSSat’s 45° (phase angle 135°) solar exclusion.

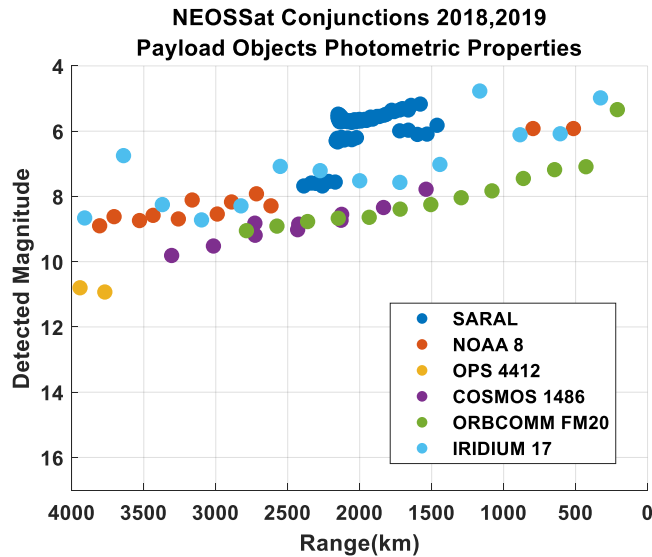
An observing campaign to characterize space objects approaching NEOSSat was performed. Close approaches forecasted by Celestrak’s SOCRATES [5] conjunction forecasting web service were used to plan observations on small to large objects making passes with NEOSSat. Celestrak’s use of a larger screening volume than 18 SPCS enabled frequent observing opportunities on approaching secondaries easing NEOSSat planning operations whereas 18 SPCS’ tighter screening volume (0.5 km radial for NEOSSat) reduces the number of conjunction events available for planning observations. Celestrak’s forecasts allows NEOSSat’s astronomy mission to be uninterrupted during its exoplanet transit experiments and fits easily with the routine task planning cycle. Table 1 identifies the objects observed by NEOSSat during their conjunctions.

Table 1 – Close approach objects observed by NEOSSat

TCA (JDAY)	TCA (UTC)	Name	Secondary SSC#	Type	RCS Size	Approach Angle (deg)	Relative Velocity (km/sec)	Miss distance (km)
2018-179	03:15:56	Orbcom B8	25416	PAYLOAD	Medium	100.6	11.49	2.99
2018-179	07:43:28	Iridium 17	24870	PAYLOAD	Large	47.6	6.02	4.874
2019-060	-	SARAL	39086	PAYLOAD	Large	-	-	-
2019-105	21:03:41	Cosmos 1275	13487	DEBRIS	Small	139.3	14.00	4.810
2019-107	18:22:18	FengYun1C	30109	DEBRIS	Small	142.9	14.21	6.236
2019-116	03:51:48	NOAA 8	13923	PAYLOAD	Large	138.2	13.91	4.81
2019-117	05:55:23	Transit 9	801	PAYLOAD	Large	81.08	9.7	56.24
2019-117	20:02:22	CZ-4 Deb	26294	DEBRIS	Medium	113.18	12.45	2.566
2019-118	08:56:24	Cosmos 1486	14240	PAYLOAD	Large	60.75	7.55	2.026
2019-118	01:44:01	CZ-4 Deb	20904	DEBRIS	Small	73.79	8.96	4.708
2019-123	20:56:56	Cosmos 1275 Deb	13026	DEBRIS	Small	135.80	13.85	1.957
2019-124	06:55:18	Cosmos 2251 Deb	34128	DEBRIS	Small	85.56	10.13	5.10
2019-125	14:00:11	Worldview-2 Deb	43368	DEBRIS	Small	92.85	10.82	23.46

Note: Four (4) additional debris objects were not detected by NEOSSat and were suspected to be fainter than NEOSSat’s detection limit

Fig. 6 and Fig. 7 show the detected photometric characteristics of secondary objects observed by NEOSSat prior to conjunction. The figures are differentiated by *Payload* and *Debris* classes due to inherent object size emphasizing their differing magnitudes ( $M_v$ ). In both cases, objects were initially observed up to 4000 km from NEOSSat down to 250-500 km range. SARAL is a special case where it flew with NEOSSat for several nearly coplanar orbital revolutions causing the appearance of densely packed photometric data<sup>1</sup>. *Payloads* tend to span magnitude ranges of  $M_v \sim 4.8-11$  and have relatively monotonically increasing light curves. An exception is Iridium 17 which appears to be rotating as glinting behavior is observed in its light curve. In Fig. 7, debris objects span magnitude ranges of  $M_v \sim 9-16$  and tend to have much higher variability likely due to their arbitrary shape and orientation.



**Fig.6.** Photometric characteristics of conjuncting *Payload* objects observed by NEOSSat

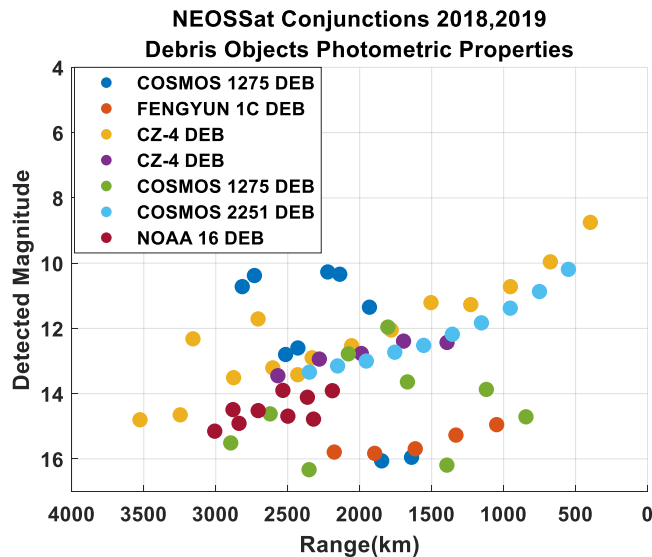


**Fig.7.** Photometric characteristics of close-approaching *Debris* objects observed by NEOSSat

<sup>1</sup> SARAL was not observed during closest approach but is included in Fig.6 to illustrate the photometry of an object with a near zero approach angle appears with respect to a LEO observer.

Comparison of Fig. 6 and Fig. 7 highlights an operational consideration when observing small debris objects prior to TCA. Debris objects were detected by NEOSSat’s image processing system after they advanced approximately ~1000 km *closer* to NEOSSat compared to the much brighter Payload class of objects. This is understandable given that NEOSSat’s image processing system’s sensitivity is  $M_v 16$ . Debris objects must advance closer and brighten above NEOSSat’s detection limit in order to be detected. Operationally, this further lessens the amount of time to acquire data on debris objects, update orbits and make a maneuver decision if a satellite faces a real-life conjunction scenario. An additional 4 debris objects were attempted during the campaign, but no detections were made. This suggests that these objects were simply too faint to be detected by NEOSSat’s instrument.

Given that debris avoidance in the few minutes leading up to TCA is a challenging and unlikely approach to collision mitigation, another approach to secondary observation is described in the following section.

#### 4. A HALF-ORBIT OBSERVING STRATEGY BY AUGMENTING PRE-TCA ORBIT STATE

Conjunctions tend to be envisaged as spontaneous, random events where two orbiting objects closely pass one another. Objects conjuncting with NEOSSat are mostly in circular orbits (see Fig. 8) making the kinematics of conjunctions somewhat predictable and, fortuitously, increases the number of observing opportunities for NEOSSat to observe the secondary prior to TCA. Most conjuncting secondaries have a “lead-up” phase prior to conjunction with NEOSSat where the secondary makes multiple, diminishing range approaches with NEOSSat at the *half-orbit* intersections prior the closest pass at TCA. These opportunities are created due to the slight difference in orbital periods between NEOSSat and the secondary establishing a synodic period of  $T_{synodic} = T_1 T_2 / (T_1 - T_2)$  where  $T_1, T_2$  are the orbital periods of the objects.

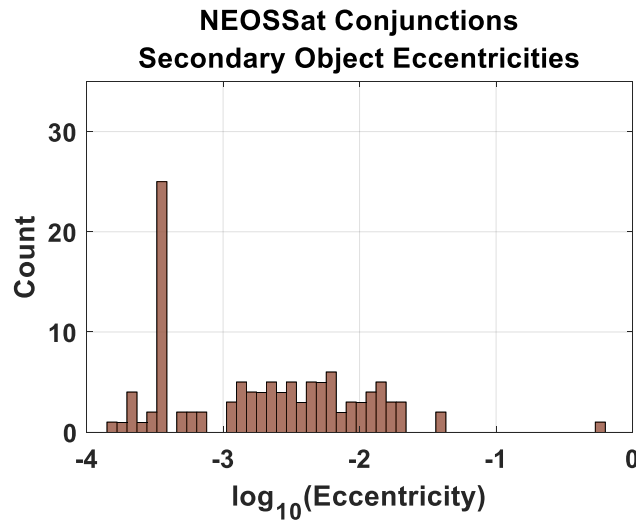


**Fig.8.** Eccentricities of conjuncting objects where a CRAMS message was produced for NEOSSat. Most of the objects have eccentricities less than 0.01. The spike at  $\log_{10}(\text{eccentricity}) \approx -3.5$  is due to cataloged, but “unknown” origin objects.

Two years of NEOSSat conjunction data taken from the CSA’s Conjunction Risk Assessment and Management System (CRAMS) [3] database was analyzed seeking conjunctions that could have been observed in by NEOSSat prior to TCA. CRAMS data includes TCA, the secondary object’s Space Surveillance catalog number, range, errors and other metadata. Each conjunction was modelled in Satellite Tool Kit using an analysis time period three days prior to TCA. NEOSSat’s observing constraints [4] were then applied to determine intervals of visibility. A further constraint was enforced such that the secondary’s phase angle was constrained to less than 90 degrees to ensure the secondary was fully Sun-illuminated increasing the likelihood of detection of smaller debris objects.

Fig. 9 shows NEOSSat’s first observing opportunities on the secondary objects prior to TCA. The first opportunities tend to spike from 0.04 to 0.12 days indicating that ~96% of NEOSSat’s conjunctions are visible with a lead time of

½ orbital revolution or more. 75% of the conjunctions had a lead time of more than 1 orbital revolution. Approximately 4% of the conjunctions had an observing lead time less than ½ orbital revolution and corresponded to the “Unknown” object population in LEO. The *lead-up* phase generally offers multiple opportunities to observe the secondary in NEOSSat’s near dawn-dusk sun synchronous orbit. If NEOSSat was equipped with an image processing and maneuvering capability, it is feasible that an autonomous debris observing strategy could be attempted.

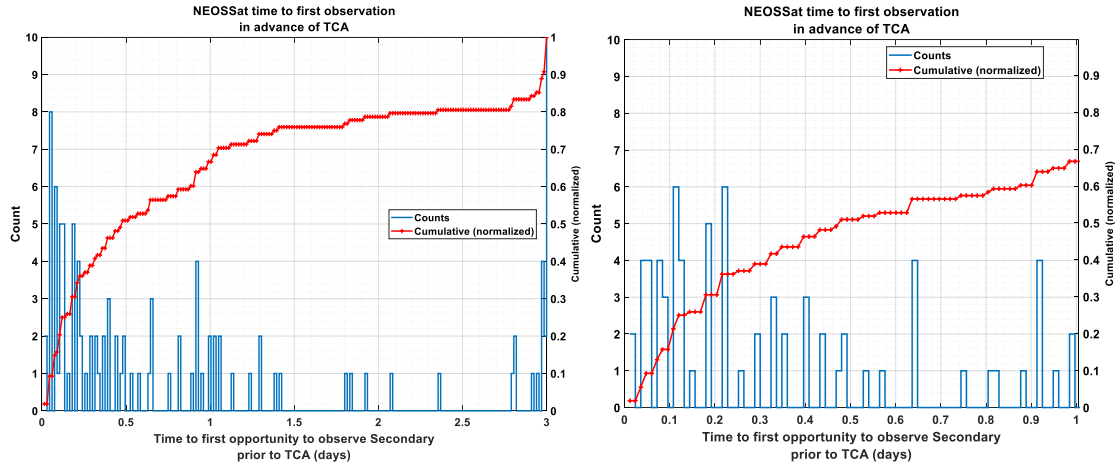


**Fig.9 (left):** Observing opportunities on secondary objects from NEOSSat prior to TCA. **(Right):** Same data showing the accesses from zero to one day of lead time.

### 5. HALF-ORBIT OBSERVING STRATEGY AND ORBIT ESTIMATION FINDINGS

Recognizing that conjuncting objects are often visible in the multiple half-orbits prior to TCA, NEOSSat conducted short observing campaigns on two conjuncting debris objects in the orbital revolutions prior to TCA. The first was a debris objects from a Japanese H-2A rocket (SSC# 43069, COSPAR: 2017-082E) orbiting Earth with an apogee and perigee of 787x742 km. This object is listed as a small (< 0.1 m<sup>2</sup>) radar cross section suggesting it has a characteristic length of ~0.3 meters. NEOSSat made several close approaches with this object in the lead-up to its conjunction on 2 June 2019 20:02:54 and safely passed the object with a miss distance of 3.05 km. As this object’s miss distance was well outside of the screening volume used by 18 SPCS, no CDM or CRAMs analysis was available. While this conjunction had a nearly zero-risk of collision, it offered an opportunity to test the half-orbit observing strategy prior to its TCA on a bright debris object for orbit estimation. Fig. 10 (left) shows the pass geometry at TCA while Fig. 10 (right) shows the close approach nodes marked over Earth’s North and South poles.

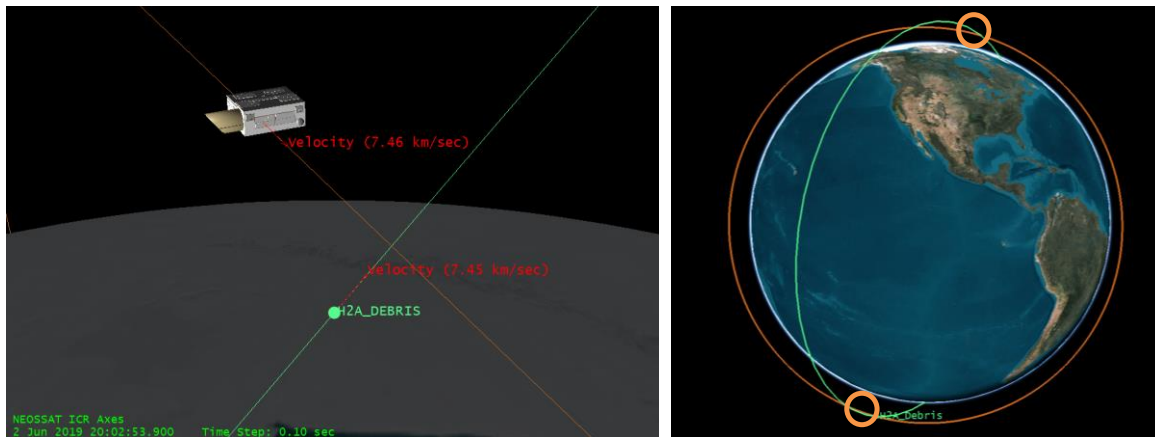


**Fig.10. (Left):** Pass geometry of the H2A debris object with NEOSSat. **(Right):** Intersections of the debris object’s orbit with NEOSSat’s orbit over the North and South poles (marked)

Four observing opportunities were available on the H2A debris prior to TCA and are shown in Fig. 11a. Photometric measurements collected by NEOSSat are shown in Fig. 11b at intervals of 2 orbits, 1 orbit, and the half-orbit prior to TCA. The object was also observed during the terminal approach phase ( $t=0$  in Fig. 11). The brightness range of the debris object spans 10<sup>th</sup> to 12<sup>th</sup> magnitude suggesting that it is quite reflective. During the terminal pass, the object's brightness expands from 9<sup>th</sup> to 13<sup>th</sup> magnitude due to the longer window of observing opportunities available at that time. The absence of data at  $t=150$  mins is due to NEOSSat's attitude control system running its momentum dumping process, hence no data was collected. NEOSSat's momentum dumping process [6] is not typical of most satellites in LEO therefore this observing interruption would unlikely be an impediment for other satellites if they could observe the approaching secondary.

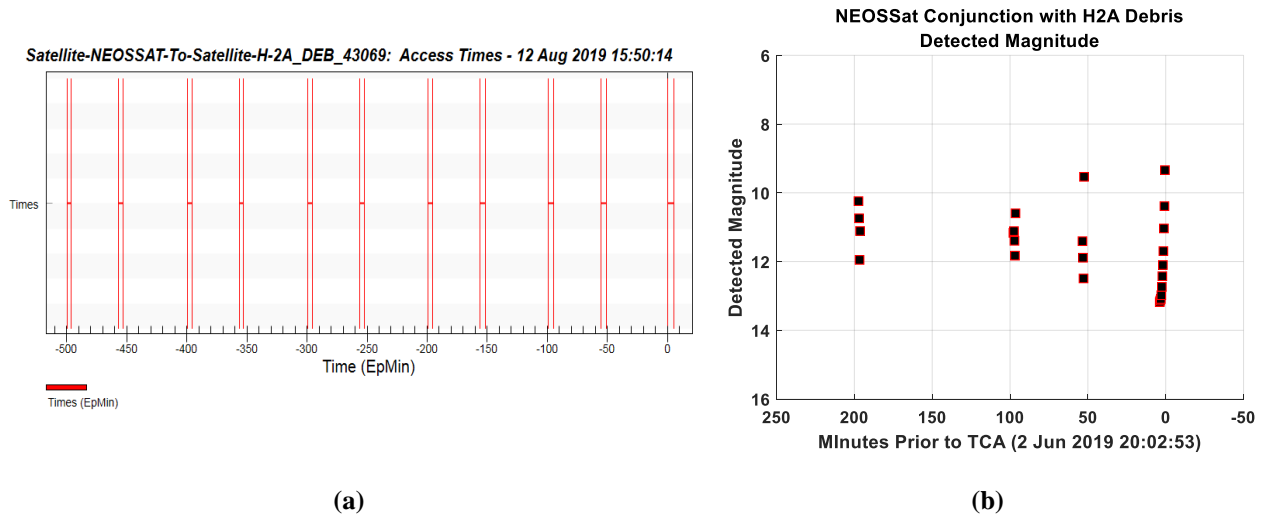


**Fig.11 (a):** NEOSSat viewing opportunities on the H2A debris prior to TCA. **(b):** NEOSSat photometry of the H2A debris taken during the orbital opportunities 200 minutes prior to TCA. Note the reversed direction of the time axis where the conjunction occurs at  $t=0$ .

To mimic NEOSSat self-estimating the orbit of the secondary using space-based optical measurements, a state and covariance was initialized for the H2A debris mimicking the typical orbital uncertainties of debris objects assessed by the CRAMS system. The H2A debris' initial position covariance was set to  $P_{Debris} = \text{diag}(35^2, 1000^2, 10^2)$  m<sup>2</sup> and NEOSSat's to  $P_{NEOSSat} = \text{diag}(10^2, 65^2, 10^2)$ . Ground processing of tracking data used NEOSSat's right ascension and declination measurements to update the state and covariance using Orbit Determination Tool Kit's (ODTK) [7] extended Kalman filter. ODTK's force model was set to a 21x21 gravity field, object mass of 2 kg and 0.1 m<sup>2</sup> cross sectional area for solar radiation pressure and drag force modeling.

Fig. 12 shows the change in the H2A debris' position uncertainty after all NEOSSat angles-only tracking data was added to the filter. Fig. 13 shows the same covariance data on a logarithmic scale emphasizing the order-of-magnitude changes of the H2A's position uncertainty in all three flight axes. Radial and in-track position uncertainties diminish significantly during NEOSSat's observations to the 10 and 30-meter level respectively. However, the H2A debris' cross-track uncertainty appears unaffected by NEOSSat's measurements. This appears to be due to the relatively high degree of positioning knowledge assumed in the a-priori covariance (10 meters cross-track positioning uncertainty) and the projected geometry of NEOSSat's observations with respect to the flight axes of the secondary.

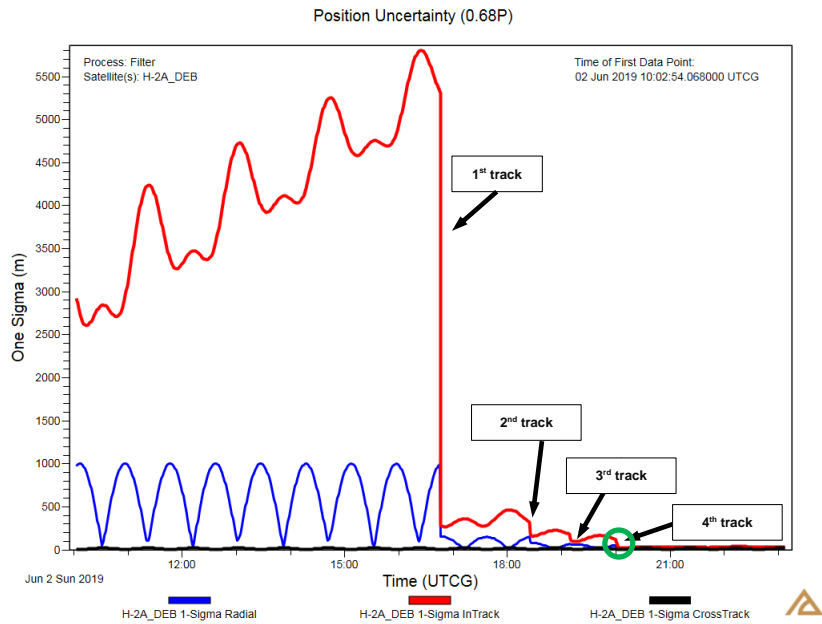


**Fig.12.** H2A debris position uncertainty with NEOSSat tracking data used to improve positional knowledge. TCA is marked with green circle. Radial, in-track and cross-track position uncertainty is marked with blue, red and black lines respectively,

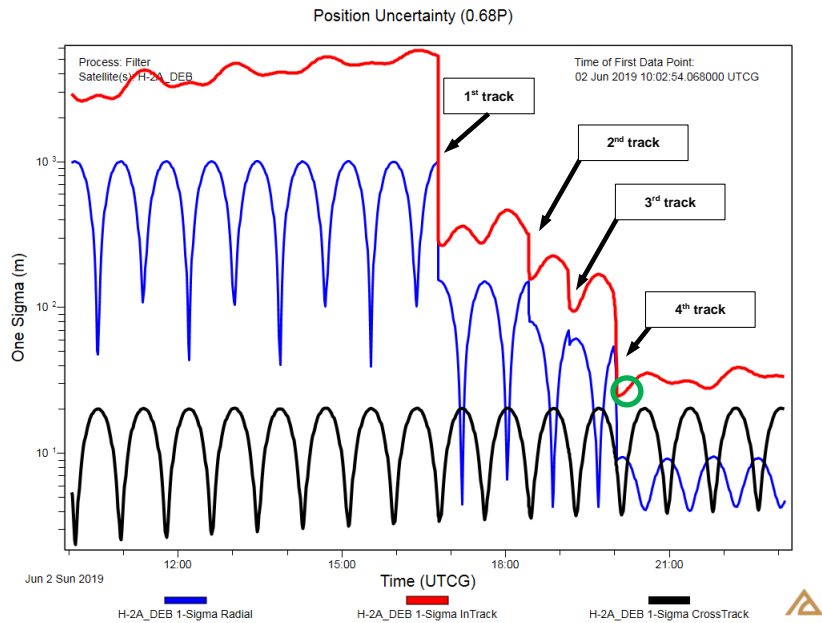


**Fig.13.** H2A debris position uncertainty as above, logarithmic scale

Fig.14 shows the covariance during the terminal phase of the H2A debris' closest approach with NEOSSat. The in-track and cross-track uncertainties show continually improving positioning knowledge when NEOSSat data was added to the filter prior to TCA. At 20:02:23 the in-track and radial position uncertainties are 25 m and 9 m respectively. The cross-track uncertainty remains unchanged even during the terminal phase of the conjunction.

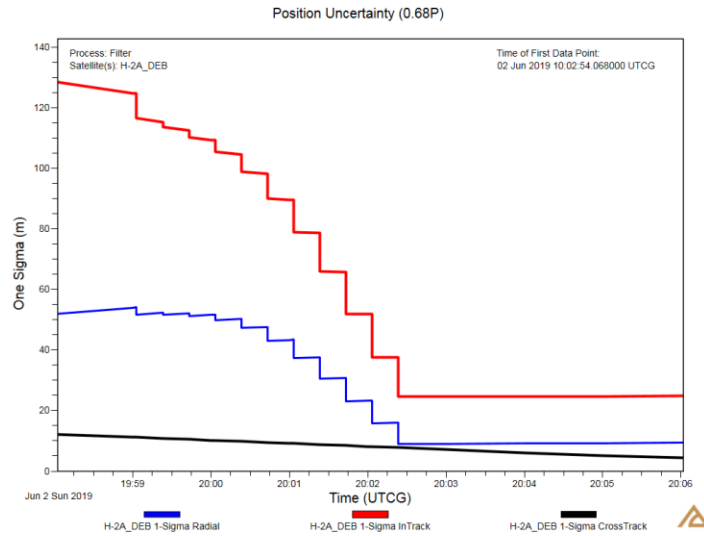


**Fig.14:** H2A position uncertainty during the terminal phase just prior to TCA at 20:02:54. Note that the cross-track uncertainty (black) is unaffected by the addition of space-based tracking data, whereas radial (blue) and in-track (red) position knowledge improves when measurement data is processed by the filter.

## 6. OBSERVATIONS OF AN OBJECT DURING A CRAMS-BASED WARNING

This case examines a more realistic conjunction where a debris object was forecasted to approach NEOSSat within 18 SPCS’ conjunction screening volume. A Conjunction Data Message was formed and the risk was evaluated by the Canadian Space Agency’s satellite operations team. The conjunction of CZ-4 debris (SSC# 26294, COSPAR: 1999-057GG) was forecasted to occur on 27 Apr 2019 20:02:21.789 UTC with a miss distance of 1.08 km (see Fig. 15a). This object had a relatively low PoC given the relatively large miss distance, however the object was considered to be representative of a realistic debris conjunction and subsequently chosen for tracking. Photometric observations during the orbit prior to TCA (1<sup>st</sup> track) and during the terminal phase (2<sup>nd</sup> track) are shown. The object tends to be  $M_v$  14 when it enters NEOSSat’s detection limits and can brighten by several magnitudes to  $M_v$  7.

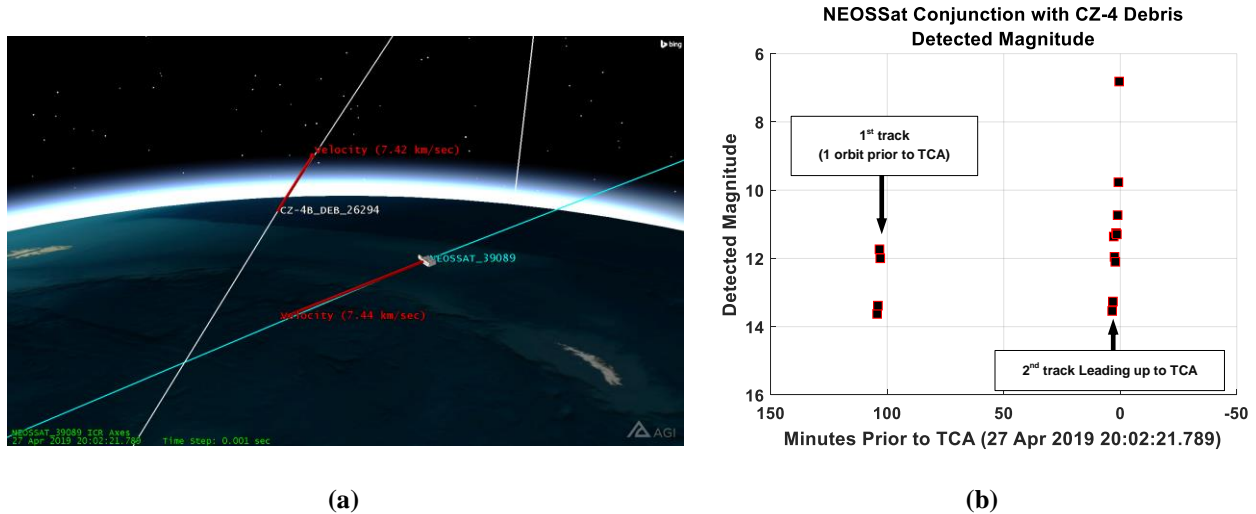


**Fig.15 (a):** NEOSSat conjunction geometry with the CZ-4 debris. **(b):** NEOSSat photometry on the CZ-4 debris taken during 100 minutes and up to 4 minutes prior to TCA ( $t=0$ ).

A state and covariance for the CZ-4 debris was provided by 18 SPCS three days prior to TCA. This state was used to initialize the orbit estimation process using the ODTK model described in the previous section. NEOSSat’s space-based measurements were used to update this a-priori state estimate. Fig. 16 shows the object’s position uncertainty, in a non-dimensionalized<sup>2</sup> scale relative to the radial position uncertainty. Significant improvement of the in-track (red), and minor radial (blue) position knowledge occurs after processing NEOSSat’s 4 measurements during the orbit prior to TCA and during the terminal phase. As shown in the previous section, NEOSSat’s observing geometry did not show significant cross-track position improvement when NEOSSat’s measurements were added to the filter. NEOSSat’s angular measurement noise (~4 arcseconds), combined with the oblique observing geometry on the secondary object, has a negligible influence on the cross-track state update when observed at ranges less than 4000 km.

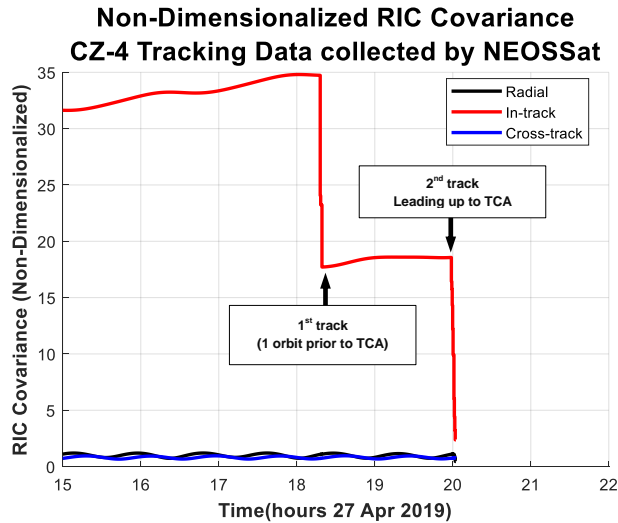


**Fig.16:** CZ-4 position uncertainty after NEOSSat observations were processed by the filter. In-track positioning knowledge improves significantly. Note non-dimensionalized scale is relative to the initial radial position uncertainty.

To mimic the case where a space-based sensor independently assesses the risk of conjunction by observing the secondary one full orbit prior to TCA, the filter was run with the 2<sup>nd</sup> track of observations ignored. The new state and covariance was propagated to TCA and a new PoC computed using Foster’s conjunction theory [8]. Table 2 shows the change in the PoC after NEOSSat’s observations updated the orbit. While this example represented a very low initial risk of collision, a sizeable reduction in PoC was found with the short, 4-observation tracklet acquired in the orbit prior to TCA.

Table 2 – Probability of Collision for CRAMS warnings due to NEOSSat-collected orbital data

	Time to TCA (days)	log <sub>10</sub> (PoC)	Miss Distance (m)
1 <sup>st</sup> Warning	6.8	-111	814
10 <sup>th</sup> Warning	3.8	-120.07	1082
10 <sup>th</sup> Warning + NEOSSat observations	3.8	-141.2	1110

<sup>2</sup> Covariance information is non-dimensionalized to preserve privacy of information provided by 18 SPCS.

Further work is required to determine the viability of this approach. The CSA is monitoring NEOSSat conjunctions with PoCs exceeding the CSA's action criteria ( $10^{-6}$ ) to enable continued observations in this area.

## 7. SUMMARY AND CONCLUSION

Space-based optical measurements of orbiting objects conjuncting with a LEO satellite observer were characterized by exploiting the near constant bearing, decreasing range observing geometry possible from a space-based platform. As NEOSSat is unable to perform on-orbit orbit estimation of other space objects, tracking data was downloaded and processed using ground-based SSA image processing and orbit estimation tools to determine viability of independent collision assessment using a Conjunction Data Message as a cue. It was found that a small sun-synchronous space surveillance telescope can optically detect the rapid advance of space objects prior to TCA if the secondary is Sun-illuminated and is elevated above Earth's limb such that astrometry can be performed on the space surveillance imagery. Both payload and debris objects were characterized in LEO with detections beginning at 4000 km range and rapidly reducing to 250 km range with apparent magnitudes spanning  $M_v \sim 4.8-11$  for payloads and  $M_v \sim 9-16$  for debris within a 4-minute timescale. Four debris objects were undetected during this campaign and were suspected to be too faint for detection by the NEOSSat instrument or not in field due to orbit uncertainty. Rapid range-induced brightening was observed for all conjuncting objects with one object showing some evidence of rotational behavior. Payloads (large) conjuncting objects were detectable up to 4000 km from NEOSSat. However, smaller debris objects required them to advance toward NEOSSat by an additional 1000 km in order to brighten enough to be inherently detectable by NEOSSat's image processing system.

A short investigation of the viability of orbit updates using space-based angles only tracking data was also performed. Since most space objects conjuncting with NEOSSat have near circular orbits, multiple repeat opportunities to observe the secondary prior to TCA is possible. An observing strategy employing opposition observations during the  $\frac{1}{2}$  orbit approaches prior to TCA helps increase the likelihood of detection of smaller objects. Observation processing on two different conjuncting space objects prior to TCA show marked improvement in the in-track position knowledge and partial improvements in the radial direction. Cross-track positioning knowledge showed little to no improvement in both tested cases. This is due to the NEOSSat's measurement uncertainty and the oblique pass geometry of the secondary during observation. A test case where the secondary was observed a full orbit prior to conjunction showed a sizeable reduction in the PoC. This suggests that this observational technique could be applied in real-world conjunction scenarios if a conjunction warning's cross-track positioning knowledge has high confidence and the object is bright enough to be detected. It appears that satellites equipped with space surveillance cameras *can* help themselves in an increasingly risky orbital debris environment.

## 8. ACKNOWLEDGEMENTS

The authors wish to acknowledge the Canadian Space Agency's Satellite Operations Centre (CSA SatOps), the Department of National Defence, Director General Space (DGSpace), and the Assistant Deputy Minister for Science and Technology (ADM S&T) for their support of the extended research mission of the NEOSSat microsatellite.

## 9. REFERENCES

- 1 18<sup>th</sup> Space Control Squadron, "Spaceflight Safety Handbook for Satellite Operators Version 1.4", Joint Functional Space Component Command, Vandenberg, Air Force Based. Accessible from Space-track.org, February 2019.
- 2 Abbasi, V., Babiker, F., Doyon, M., Golla, D., "Close Encounters of an Advanced Kind: Lessons Learned and New Approaches in Collision Risk Assessment and Mitigation", 7<sup>th</sup> *European Conference on Space Debris*, Darmstadt, Germany, 2019, <https://conference.sdo.esoc.esa.int/proceedings/sdc7/paper/1006/SDC7-paper1006.pdf>
- 3 Babiker, F., Doyon, M., Abbasi, V., "Canadian Space Agency (CSA) Collision Risk Assessment and Mitigation System (CRAMS): Sharing the Development and Operational Challenges", *SpaceOps Conference 2012*, Stockholm, Sweden, 12 June 2012, <https://doi.org/10.2514/6.2012-1297827>.
- 4 Scott, R.L., Thorsteinson, S.E., "Key Finding from the NEOSSat Space-Based SSA Mission", *AMOS Conference 2018*, Maui Economic Development Board, Maui, HI, 2018.

- 5 Kelso, T.S., “Socrates: Satellite Orbital Conjunction Reports Assessing Threatening Encounters in Space”, web application accessible from <https://www.celestrak.com/SOCRATES/>, accessed Aug 5, 2019.
- 6 Abbasi, V., Jackson, N., Doyon, M., Wessels, R., Sekhavat, P., Cannata, M., Gillett, R., Eagleson, S., “NEOSSat Recovery following Magnetometer and Torque Rod Failure”, *15<sup>th</sup> International Conference on Space Operations (SpaceOps 2018)*, Marseilles, France, 2018. <https://arc.aiaa.org/doi/pdf/10.2514/6.2018-2664>
- 7 Wright, J., “Orbit Determination Tool Kit Theory and Algorithms”, Analytical Graphics, accessible from: <https://www.agi.com/resources/white-papers/orbit-determination-tool-kit-theory-and-algorithms>, accessed 1 Aug 2019.
- 8 Foster, J.L., “The Analytic Basis for Debris Avoidance Operations for the International Space Station”, In *Proceedings of the Third European Conference on Space Debris*, 19 - 21 March 2001, Darmstadt, Germany